Mitochondria-targeting near-infrared ratiometric fluorescent probe for selective imaging of cysteine in orthotopic lung cancer mice

Xiaoyu Zhang[a,b,d], Na He[a,b,d], Yan Huang[b], Fabiao Yu[c,d,**], Bowei Li[b], Changjun Lv[a,d,**], Lingxin Chen[b,e,*]

[a] Department of Respiratory Medicine, Binzhou Medical University Hospital, Binzhou, 256603, China
[b] CAS Key Laboratory of Coastal Environmental Processes and Ecological Remediation, Yantai Institute of Coastal Zone Research, Chinese Academy of Sciences, Yantai, 264003, China
[c] Institute of Functional Materials and Molecular Imaging, College of Emergency and Trauma, Hainan Medical University, Haikou, 571199, China
[d] Medicine Research Center, Institute of Molecular Medicine, Binzhou Medical University, Yantai, 264003, China
[e] College of Chemistry and Chemical Engineering, Qufu Normal University, Qufu, 273165, China

ARTICLE INFO

ABSTRACT

Cysteine (Cys) plays significant roles in many physiological processes, although its normal concentration is maintained at the micromole level. Abnormally high levels of intracellular Cys can lead to many diseases including cancer. Recent years, many effective fluorescent probes have been developed for the selective detection of Cys against other biological thiols. Herein, we synthesized a ratiometric near-infrared (NIR) fluorescent probe **Cy-OAcr** for selective imaging of intracellular Cys. **Cy-OAcr** has a lipophilic iminium cation unit as the mitochondrial guider and an acrylate group as the Cys recognition unit as well as a fluorescence modulator for rearranging the conjugated π-electron system of cyanine fluorophore. Upon detection of Cys, there occurs a significant absorption and fluorescence spectral shift, which are desirably beneficial for ratiometric detection. This probe has high sensitivity and selectivity for Cys detection over glutathione (GSH), homocysteine (Hcy), and other biomolecules with a low limit of detection at 0.09 μM. Probe **Cy-OAcr** is capable to detect and image Cys in three living cancer cell lines and their corresponding tumor-bearing mice models. More importantly, we successfully apply this fluorescent probe to evaluate the level of Cys in orthotopic lung cancer model. Imaging analyses reveal that the probe can discriminate tumor lesions from normal tissues, indicating its significant potential applications for clinical auxiliary diagnosis of cancer.

1. Introduction

As an important biological thiol, cysteine (Cys) plays vital roles in the biological organisms. Once incorporated into cells, most of Cys is immediately involved in the synthesis of glutathione (GSH). However, Cys holds an independent redox pool to regulate mitochondrial dynamic antioxidant defenses compared to the antioxidant system of GSH [1]. The severe level changes of intracellular Cys will result in many diseases. The abnormally high concentrations of Cys has relationship with cardiovascular disease, neurotoxicity, Alzheimer's disease, and Parkinson's disease, while the deficiency will cause edema, alopecia, and liver damage, although the actual cause of those diseases is still debatable [2]. Especially in cancer cells, the change of Cys concentration is much higher than that of GSH [3]. That is, cancer tissue has

significantly higher levels of Cys than adjacent normal tissue [4]. The determine of the levels of intracellular Cys can potentially discriminate tumor lesions from adjacent more normal tissue. However, the detection of Cys is always challenged by GSH and homocysteine (Hcy) because of the similar chemical structure and properties (Supporting information, Fig. S2) [5,6]. Moreover, the levels of Cys, Hcy and GSH in cells are very different. GSH is the most abundant non-protein thiol in cell, the concentration is at about millimolar levels. But the contents of Cys and Hcy are at about micromole level [1,7]. Therefore, it is full of challenges to develop the selective and sensitive detection method of Cys against other biothiols such as Hcy and GSH.

Previous efforts on Cys detection, including high performance liquid chromatography (HPLC) [8], mass spectrometry (MS) [9], HPLC-MS [10], immunoassay [11], and capillary electrophoresis separations

---

* Corresponding author at: CAS Key Laboratory of Coastal Environmental Processes and Ecological Remediation, Yantai Institute of Coastal Zone Research, Chinese Academy of Sciences, Yantai, 264003, China.
** Corresponding authors at: Medicine Research Center, Institute of Molecular Medicine, Binzhou Medical University, Yantai, 264003, China.
E-mail addresses: fbyu@yic.ac.cn (F. Yu), lucky_lcj@sina.com (C. Lv), lxchen@yic.ac.cn (L. Chen).

[12,13] methods, often involve time-consuming and complicated separate steps [14]. Fluorescent probes combined with imaging techniques has now become indispensable chemical tools for the detection of reactive biological small molecules in living biosystems due to the high sensitivity and unrivaled spatiotemporal resolution [15,16]. Current fluorescent probes are mainly designed for specific identification of Cys, Hcy and GSH in cells [17–31]. The fluorescence response mechanisms involve Förster resonance energy transfer mechanism [32–34], photoinduced electron transfer mechanism [35–37], intromolecular charge transfer mechanism [38,39], as well as aggregation-induced emission mechanism [40,41], and so on. The type of reaction detection mechanisms are commonly adopted Michael addition [42], cyclization reaction [43], cleavage reaction [44], conjugated addition-cyclization reaction [45], cascade reaction [46] and substitution-rearrangement [34].

Although many fluorescent probes have made a significant contribution to the detection of Cys, there still exist many issues to be solved. The fluorescent probes whose emission locate in the ultraviolet or visible region are limit by penetration and photobleaching for bioimaging in cells, particularly in vivo [47,48]. The reported probes which based the BODIPY and coumarin fluorophores have failed to target mitochondria for Cys detection [17,28,32]. More importantly, most of these fluorescent probes often achieve Cys detection only at the cell level [16,17,30,49]. In order to further reveal the roles of Cys in pathogenesis and physiology, it is necessary to design and synthesize an effective fluorescent probe for in real-time imaging of the accurate distribution of Cys in cells and in animal models. Moreover, the NIR fluorescence can maximize tissue penetration while minimizing the absorbance of heme in hemoglobin and myoglobin, water, and lipids, therefore, the NIR fluorescent probes are more desirable for in real-time imaging the distribution of Cys in cells and in vivo [50–52]. In order to be satisfied precise fluorometric analyses under biological conditions, the ratiometric probes which employ the ratio of the emission intensity at two different wavelengths are more preferred, because interferences from uneven loading or the inhomogeneous distribution of fluorescent probes in cells can be reduced [53,54]. After scanning the above mentioned issues for Cys detection, Yoon et al reported a near-infrared ratiometric fluorescence probe CyAC for the detection of Cys in cells and in vivo [55].

Herein, in view of the excellent performance of CyAC, we further synthesized a ratiometric NIR fluorescent probe **Cy-OAcr** for the detection of mitochondrial Cys over GSH and Hcy in cells and in orthotopic lung cancer mice. The probe **Cy-OAcr** was able to quickly react with Cys and produce a shift in fluorescence emission profile, meanwhile avoiding the interference from other small endogenous reactive small molecules. The probe could be used to discriminate Cys levels in diffrent types of cancer cell lines, and the iminium cation of this fluorophore platform could facilitate the probe accumulating in mitochondria. To the best of our knowledge, we first applied a Cys fluorescent probe for imaging of tumor lesions in orthotopic lung cancer models. We envisioned that the probe **Cy-OAcr** could contribute to further understanding the roles of Cys in physiological and pathological condition. And Cys might be a potential biomarker for the clinical diagnosis of tumor.

2. Experimental section

2.1. Synthesis of the probe Cy-OAcr

2.1.1. Synthesis of compound 2 (Keto-Cy)

To a solution of compound 1 (0.512 g, 1.0 mmol) and sodium acetate (0.164 g, 2 mmol) dissolved in anhydrous DMF (10 ml) under argon protection. The reaction mixture was reacted at 50 °C for 12 h [56,57]. The crude product was extracted and washed by water : dichloromethane = 1 : 1 (v/v) three times. The solvent was removed under reduced pressure. The resulting solid was purified by flash chromatography using dichloromethane : ethyl acetate = 10 : 1 (v/v) as eluent to afford dark red solid (0.43 g, yield: 87%). ^{1}H NMR (DMSO-D$_6$, 500 MHz) δ (ppm): 7.96-7.93 (d, 2 H), 7.34-7.33 (d, 2 H), 7.22-7.19 (m, 2 H), 6.92-6.89 (m, 4 H), 5.50-5.47 (d, 2 H), 3.83-3.79 (q, 4 H), 2.58-2.55 (t, 4 H), 1.76-1.74 (m, 2 H), 1.57 (s, 12 H), 1.18-1.13 (m, 6 H). ^{13}C NMR (DMSO-D$_6$, 125 MHz) δ (ppm): 188.26, 164.17, 145.11, 142.53, 133.23, 129.36, 123.81, 119.59, 109. 73, 98.84, 50.08, 37.94, 29.06, 25.01, 20.05, 9.94. HRMS (ESI$^+$): m/z C$_{34}$H$_{40}$N$_2$O calcd. 492.3141, found [M + H]$^+$ 493.3142.

2.1.2. Synthesis of compound 3 (Cy-OAcr)

To a solution of acryloyl chloride (0.905 g, 10 mmol) in anhydrous dichloromethane (10 ml) under argon protection, compound 2 (0.493 g, 1 mmol) was dripwisely added [55]. The reaction mixture was lasted at 0 °C for 1 h, and then heated to 25 °C for 12 h. The crude product was washed by water three times. The solvent was removed under reduced pressure. The resulting solid was purified by flash chromatography using ethyl acetate : methanol = 1 : 1 (v/v) as eluent to afford green solid (0.498 g, yield: 91%). ^{1}H NMR (DMSO-D$_6$, 500 MHz) δ (ppm): 7.65-7.61 (m, 3 H), 7.45-7.44 (m, 2 H), 7.29-7.27 (m, 2 H), 6.88-6.72 (m, 2 H), 6.49-6.47 (m, 1 H), 6.28-6.25 (m, 3 H), 6.14-6.11 (m, 1 H), 5.90-5.88 (m, 1 H), 4.27-4.22 (m, 4 H), 2.76-2.71 (m, 4 H), 1. 55 (s, 12 H), 1.33-1.30 (m, 8 H). ^{13}C NMR (DMSO-D$_6$, 125 MHz) δ (ppm): 171.90, 171.61, 167.35, 163.79, 158.73, 142.12, 141.54, 139.78, 136.51, 131.12, 130.05, 129.10, 127.11, 125.47, 123.02, 121.36, 111.74, 100.96, 49.25, 37.67, 27.83, 24.19, 20.97, 12.65. HRMS (ESI$^+$): m/z C$_{37}$H$_{43}$N$_2$O$_2$$^+$ calcd 547.3319, found [M] 547.3320.

2.2. Cell culture

The A549 cell line, H1650 cell line and PC9 cell line were purchased from Chinese Academy of Sciences stem cell bank/stem cell technology platform. A549 cell line were incubated in F-12 K (Invitrogen, 21127-022) supplemented with 10% fetal bovine serum (FBS, gibco), H1650 cell line were incubated in RPMI (gibco, 11875-093) supplemented with 10% FBS, PC9 cell line were incubated in DMEM (HyClone, SH30022.01) supplemented with 10% FBS. The cells grew in the incubator (37 °C, 5% CO$_2$).
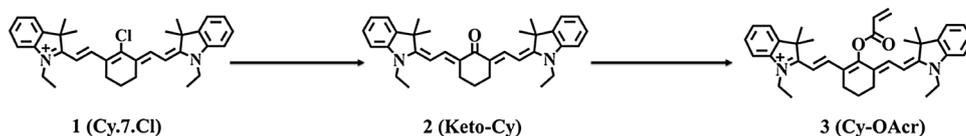
2.3. Construction of tumor-bearing mice model

BALB/c nude mice, female, 4 weeks old, were provided by Changzhou Cavens Lab Animal Co. Ltd. A549 cell line, H1650 cell line and PC9 cell line digested into suspension with concentration of 1×10^7 /ml in serum-free medium for cell xenografts. Until the diameter of tumor reached about 6 mm can be experiment.

2.4. Construction of orthotopic lung cancer mice model

SPF grade FVB male mice purchased from Beijing Vital River Laboratory Animal Technology Co., Ltd. 6 weeks old, body weight 20 ± 2 g. Mice received i.p. injections of 8% urethane (dissolved in saline) at a dose of 0.01 ml g^{-1} twice a week for 5 weeks [58]. Then it would take three months for the devlopment of orthotopic lung cancer lesions. The weights of mice were monitored once a week when the model was started, and the growth status of mice was observed every day.

2.5. Cell counting Kit-8 (CCK-8) experiment

The growth adherent cells were digested into cell suspensions. The number of cells in the prepared cell suspension was counted by cell counting plates. Then, the cells were inoculated into 96 holes and the cell suspension 100 μl was added per hole. 96-well cell culture plate were cultured in a cell incubator for 24 h. Different concentrations (0–100 μM) of **Cy-OAcr** (10 μl) were added into the culture plate. The

Scheme 1. Synthetic route of probe **Cy-OAcr**. a) sodium acetate, anhydrous DMF, 50 °C 12 h, 87%; b) acryloyl chloride, anhydrous CH₂Cl₂, 0 °C 1 h, then 25 °C 12 h, 91%.

culture plate was incubated in incubator for 24 h. Add 10 μl CCK-8 of solution to each hole (notice not to generate bubbles in the hole). The 96-well cell culture plate was incubated in the incubator for 30 min and then determined the absorbance value by microplate reader at 450 nm.

2.6. Confocal laser scanning microscope imaging experiment

The cells which grew well were digested into cell suspension and inoculated into the Petridishes (Φ = 20 mm). The cells were incubated in the incubator for 24–48 h and then performed the confocal imaging with an objective lens (× 60). In vitro fresh lung tissue confocal imaging with an objective lens (× 40). Fluorescence excitation and collection filters were described in the paper. Fluorescence imaging detection gain remains constant throughout the experimental process.

2.7. Flow cytometry analysis

Take logarithmic growth phase cells digested into cell suspension and inoculated into 6-well plates (define: 2.0 × 10⁵ cells/well). The 6-well plates incubated for 24 h. Then treated with **Cy-OAcr** as described in the paper. After the treatment was complete, the cells are washed with Phosphate Buffered Saline (PBS) and digested into cell suspensions suspended in fresh complete medium and for flow cytometry analyzed. Fluorescence excitation wavelength and collection wavelength described in the paper.
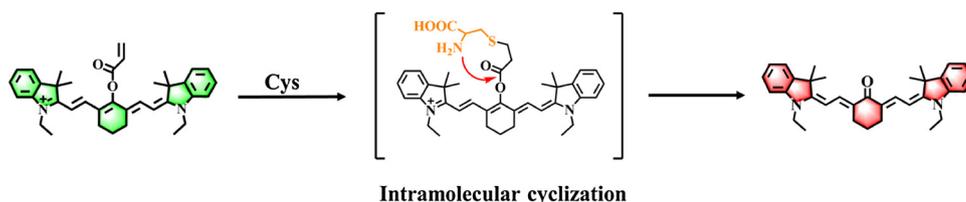
2.8. In vivo mice imaging

In vivo imaging of mice performed on Perkinelmer IVIS Lumina XRMS Series III In Vivo Imaging System. Fluorescence imaging detection gain remains constant throughout the experimental process.

2.8.1. Nude mice in vivo imaging

BALB/c nude mice (female, 4 weeks old), intratumoral injection of probe **Cy-OAcr** or NEM, after 1 h, the mice were anesthetized with isoflurane gas and then performed in vivo fluorescence imaging. Imaging includes bright field, fluorescence and X-ray. Fluorescence excitation wavelength and collection wavelength described in the paper.

2.8.2. Orthotopic lung cancer mice in vivo imaging

FVB mice (male, 6 weeks old) were administered **Cy-OAcr** through the trachea, after 15 min and 30 min, the mice were anesthetized with isoflurane gas then in vivo imaging. Imaging includes bright field, fluorescence and X-ray. Lung tissues imaging were performed after the end of in vivo imaging. Fluorescence excitation wavelength and collection wavelength described in the paper.

2.9. Ethics statement

All experimental procedures were conducted in conformity with institutional guidelines for the care and use of laboratory animals, and protocols were approved by the Institutional Animal Care and Use Committee in Binzhou Medical University, Yantai, China. Approval Number: No. BZ2014-102R.

3. Results and discussion

3.1. Design and synthesis of Cy-OAcr

Inspired by the design strategy from Yoon et al. [55] work, we strive to synthesis a ratiometric NIR fluorescent probe for the detection of Cys in cells and in vivo. As shown in Scheme 2, Ketone cyanine (Keto-Cy) is chosen as the fluorescence signal transducer. The chemical modification of a fluorescence modulator on the *meso*-position of this cyanine fluorophore will result in the change of the conjugated π-electron system, which has been proved to be an efficient approach for dominating fluorescence emission profile changes [55,59]. Moreover, the substituent on N-atom of indoline is changed to ethyl. This tiny difference of molecular structure can reduce thermal effects of NIR light, which may be beneficial for the protection of cells for the non-invasive tests [60]. *α, β*-Unsaturated acrylate (Acr) is selected as the fluorescence modulator because it could discriminate Cys, Hcy, and GSH via an unique adduct/intramolecular cyclization [61–65]. Our efforts finally result in a ratiometric NIR probe **Cy-OAcr** for the specific detection of Cys over Hcy and GSH. The synthesis routes of **Cy-OAcr** was described in Scheme 1. Ketone-type cyanine dye (Keto-Cy) was prepared from the substitution and hydrolysis reaction between heptamethine cyanine and sodium acetate in anhydrous *N,N*-dimethylformamide [66]. The incorporation of acryloyl chloride into Keto-Cy in anhydrous dichloromethane would afford the final probe **Cy-OAcr**. The related chemical structures were identified via ¹H NMR, ¹³C NMR, and HRMS. The detection mechanism of the probe **Cy-OAcr** was shown in Scheme 2.

3.2. Spectral properties and selectivity of Cy-OAcr

The absorption and fluorescence spectra of **Cy-OAcr** were examined under simulated physiological conditions (10 mM HEPES buffer, pH 7.4, 37 °C). UV–vis spectra of **Cy-OAcr** were detected after addition of Cys in HEPES (Fig. S3a). When treated with increasing concentrations of Cys (0–20 μM), the absorption peak centered at 769 nm ($\varepsilon_{769\ nm} = 1.0 \times 10^5$ M⁻¹ cm⁻¹) decreased, and a new absorption peak centered at 505 nm ($\varepsilon_{505\ nm} = 1.8 \times 10^4$ M⁻¹ cm⁻¹) emerge, respectively. The isosbestic point was at 595 nm. The color of the solution turned from green into red. The obvious color change indicated that **Cy-OAcr** potentially served as a naked-eye probe for Cys. As expected, there was a large hypsochromic spectral shift in emission profiles (Fig. 1a, b). As the
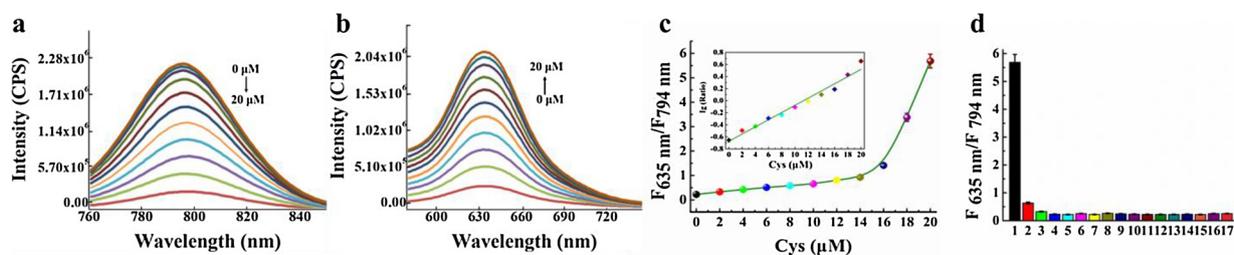

Intramolecular cyclization

Scheme 2. Molecular structure and proposed mechanism of **Cy-OAcr** for the ratiometric detection of Cys.

Fig. 1. Spectral properties and selectivity of **Cy-OAcr**. a) Dose-dependent emission spectra (λ_{ex} = 750 nm) of **Cy-OAcr** (10 μM) towards Cys. b) Dose-dependent emission spectra (λ_{ex} = 535 nm) of **Cy-OAcr** (10 μM) towards Cys. c) The fluorescence ratio signal ($F_{Ratio} = F_{635\,nm}/F_{794\,nm}$) of **Cy-OAcr** towards Cys. Inset: the linear relationship between Lg(Ratio) and Cys. d) Selectivity of **Cy-OAcr** towards different biologically reactive species. 1, Cys (0.2 mM); 2, GSH (8 mM); 3, Hcy (0.2 mM); 4, H₂S (0.1 mM); 5, Asp (1 mM); 6, Glu (1 mM); 7, Gly (1 mM); 8, Lys (1 mM); 9, BSA (1 mM); 10, NO (0.1 mM); 11, H₂O₂ (0.1 mM); 12, HOCl (0.1 mM); 13, Ca²⁺ (1 mM); 14, Fe²⁺ (0.2 mM); 15, Zn²⁺ (0.2 mM); 16, Br⁻ (0.1 mM); 17, Cl⁻ (0.1 mM). Date were recorded at 45 min. The data were shown as mean (± s.d.) (n = 7).

Cys concentration gradient increased, the fluorescence emission of **Cy-OAcr** at 794 nm (Φ = 0.076) dramatically decreased, and finally resulted in the fluorescence emission of Keto-Cy at 635 nm (Φ = 0.35). The spectral shift in emission profiles could provide an efficient ratiometric approach for Cys detection in cells and in vivo. There was a linear concentration-dependent ratiometric fluorescent response with **Cy-OAcr** towards Cys ranging from 0 to 20 μM, and the calibration curve was $LgF_{635\,nm}/F_{794\,nm} = 5.95 \times 10^{-2}$ [Cys] μM – 0.67 with a linear fitting constant r = 0.9918 (Fig. 1c). The limit of detection was calculated as 0.09 μM ($3\sigma/k$) under the experimental conditions. The results indicated that our probe could be used to detect intracellular Cys qualitatively and quantitatively. The time-dependent spectral changes of the probe showed that the release of fluorophore Keto-Cy was very fast and complete within 30 min (Fig. S3b).

As shown in Fig. 1d, when reacted with potential interference species, the probe only offered a very high level of ratiometric fluorescence emission towards Cys. Other reactive biothiols, such as GSH and Hcy displayed quite a little of fluorescence increase but far lower than that of Cys. The reasoned was attributed to that Hcy and GSH might efficient in the initial nucleophilic attack at the $\alpha,\ \beta$-unsaturated acrylate of **Cy-OAcr** but inefficient in the subsequent intramolecular cyclization. Mixture of **Cy-OAcr** with amino acid (aspartic acid, glutamic acid, glycine, and lysine), bovine serum albumin (BSA), reactive oxygen/nitrogen species and reative species (NO, H₂O₂, and HOCl), anions and cations (Ca²⁺, Fe²⁺, Zn²⁺, Br⁻, and Cl⁻) at the corresponding physiological concentrations did not induce any detectable fluorescence changes. Additionally, the addition of Cys (0.2 mM) to the mixture of Hcy (0.2 mM) and GSH (5 mM) also induced a strong increase of fluorescence ratio as the mixture of the probe with Cys only (Fig. S3c). These results showed that the probe **Cy-OAcr** was a ratiometric NIR fluorescent probe that had promising potential for the highly selective detection of Cys. Our probe should be a suitable candidate for Cys detection in the biological systems.

3.3. Cytotoxicity and mitochondrial localization

We chose human lung cancer cell lines (A549 cell line, H1650 cell line, and PC9 cell line) as cell test models, because the cancer cells have higher levels of Cys than normall cells [4]. Cys might be a potential biomarker for tumor diagnosis. Before cell experiments, we first investigated the cytotoxicity of **Cy-OAcr**. The three cell lines were cultured in 96-well plates and incubated with gradient change concentration of **Cy-OAcr** (0–100 μM) for 24 h. Then Cell Counting Kit-8 (CCK-8) solution was added and incubated for 30 min. The absorbance value at 450 nm was measured using a microplate reader. The results displayed that the probe **Cy-OAcr** had low cytotoxicity and the IC₅₀ values of A549 cells, H1650 cells, and PC9 cells were 120.12 μM, 122.19 μM and, 125.48 μM, respectively.

Mitochondria play critical roles in many physiological processes including reactive oxygen species (ROS) generation, apoptosis

initiation, and cellular proliferation regulation [67]. The functional and regulatory mitochondrial Cys modifications can modulate protein activities to cell stress [68]. But the damage and dysfunction of mitochondrion will result in cancer and multiple neurodegenerative diseases [69]. Given the important physiological functions of Cys in mitochondria, the effective imaging of mitochondrial Cys enabled us to better understand its important roles in the process of cancer development. The lipophilic iminium cation in the backbone of **Cy-OAcr** would allow the probe preferentially accumulating in mitochondria. In order to confirm the mitochondria localization ability of the probe, we employed two commonly used commercially mitochondria-specific dyes, Mito-Tracker Green and Rhodamine123, to carry out the colocalization experiments using confocal laser scanning microscope. The spectrally separated images acquired from the four dyes were estimated using Image-Pro Plus software (Fig. 2). As illustrated in Fig. 2, the fluorescence images of the probe were well merged with the fluorescence images of Mito-Tracker Green and Rhodamine123, respectively. The Pearson's correlation coefficients between our probe and Mito-Tracker Green in A549, H1650, and PC9 cells were 0.96, 0.94 and 0.97, respectively. The Pearson's correlation coefficients between our probe and Rhodamine123 in A549, H1650, and PC9 cells were 0.93, 0.95 and 0.91, respectively. We also performed intensity correlation analysis of the dyads (between the probe and Mito-Tracker Green/Rhodamine 123, respectively). The costaining analysis was based on counting the intensity of stain color-pair for each pixel, which demonstrated the intensity distribution of the two colocalization dyes. As shown in Fig. 2 (correlation), only the costain **Cy-OAcr** against mitochondrial dyes offered highly correlated plots. It should be noted that the fluorescence images of the probe were acquired from the fluorescence collection window from 610 to 700 nm, where the fluorescence emission belonged to the Keto-Cy fluorophore. We performed lysosome containing experiments to further verify the localization capability of our probe **Cy-OAcr** in mitochondria. The A549 cell line, H1650 cell line, and PC9 cell line were incubated with the probe **Cy-OAcr** for 30 min, LysoTracker Green DNA-26 for 30 min, and nuclear dye Hoechst 33,342 for 30 min, respectively. As shown in Fig. S8, probe **Cy-OAcr** had poor localization in lysosome. That was, our probe **Cy-OAcr** could exactly react with Cys in mitochondria. The above results verified that probe **Cy-OAcr** possessed excellent mitochondrial-targeting ability and could be used to detect mitochondrial Cys in living cells.

3.4. Detection of cysteine levels in different cell lines

We next investigated whether the probe **Cy-OAcr** could quickly respond to intracellular Cys. The A549, H1650 and PC9 cells were incubated with 10 μM **Cy-OAcr** for 10 min, then the cells were washed with corresponding fresh cell culture mediums. As shown in Fig. 3a, the time-dependent ratiometric changes of the probe demonstrated that the detection process was very fast and completed within 30 min. The probe **Cy-OAcr** could also be utilized for Cys detection via flow
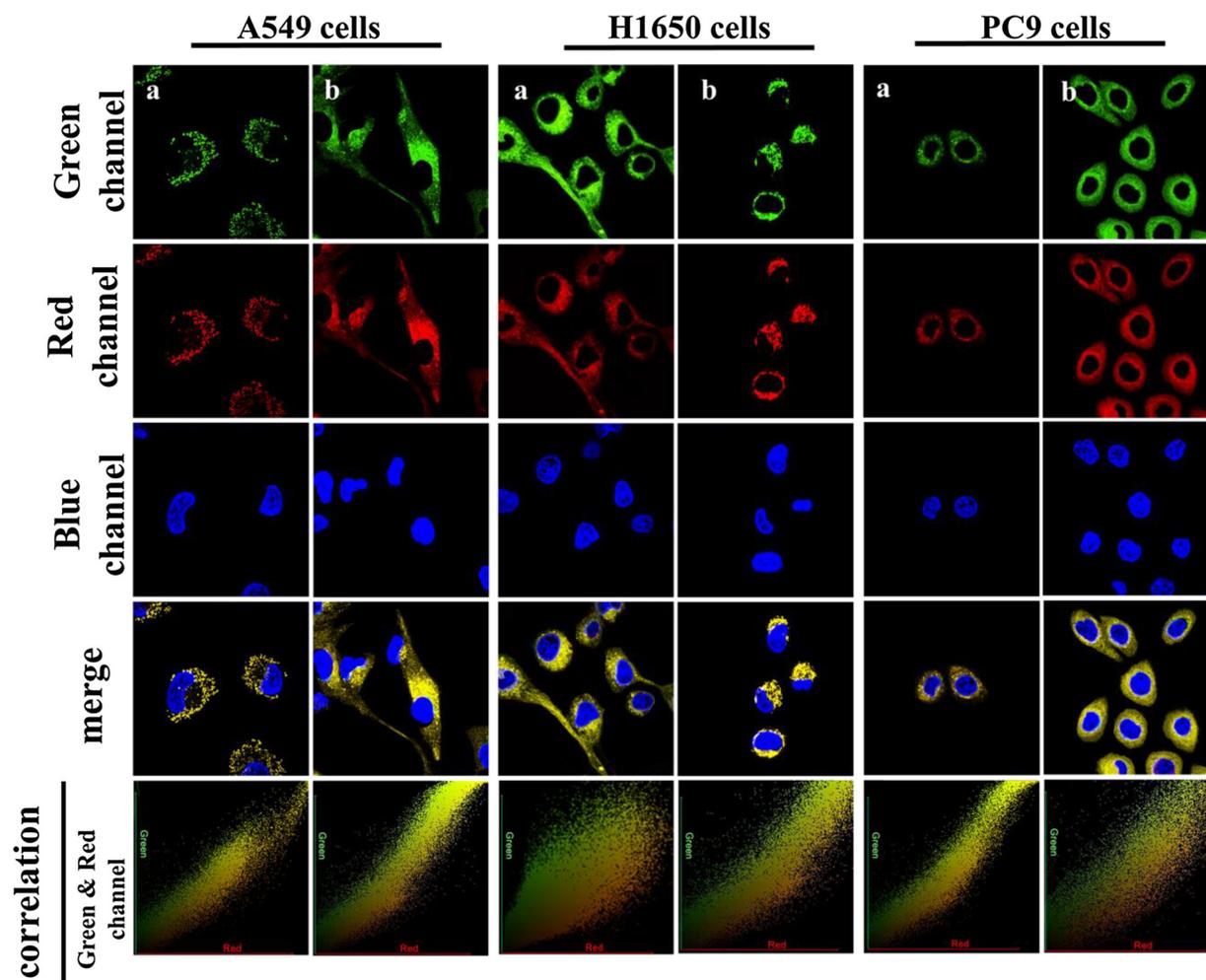
Fig. 2. Mitochondrial multicolor colocalization of **Cy-OAcr** (Red channel) with MitoTracker Green (Green channel a), Rhodamine 123 (Green channel b) and Hoechst 33,342 (Blue channel) in A549 cell line, H1650 cell line and PC9 cell line. The cells were incubated with probe **Cy-OAcr** (10 μM) for 30 min, Mito-Tracker Green (1 μg mL^{-1}) for 15 min, Rhodamine 123 (1 μg mL^{-1}) for 15 min, and nuclear dye Hoechst 33,342 (1 μg mL^{-1}) for 30 min, respectively. Green channel a: λ_{ex} = 488 nm, λ_{em} = 450–550 nm. Green channel b: λ_{ex} = 515 nm, λ_{em} = 550–600 nm. Red channel: λ_{ex} = 550 nm, λ_{em} = 610–700 nm. Blue channel: λ_{ex} = 405 nm, λ_{em} = (For interpretation of the references to colour in this figure legend, the reader is referred to the web version of this article).410–510 nm.

cytometry analysis. As shown in Fig. 3b–d the fluorescence intensities for flow cytometry analysis were collected at 0 min and 30 min. The result displayed that the fluorescence intensity of Channel 1 decreased while the fluorescence intensity of Channel 2 increased. The probe reacted completely within 30 min. The results were highly consistent with the ratio values in Fig. 3a and e. The results suggested that **Cy-OAcr** could quickly penetrate into cells and rapidly react with Cys in mitochondria.

We further performed four control cell assays to verify the selectivity of the probe **Cy-OAcr** towards Cys in cells. As illustrated in Fig. 4, the cells in group a were treated with N-ethylmaleimide (NEM) for 30 min to deplete all the intracellular biothiols, then added **Cy-OAcr** incubated for 30 min. The cells in group b, c, and d were preincubated with exogenous Cys, Glutathione monoethyl ester (GSH-MEE), and Hcy for 30 min. After washed with the corresponding fresh cell culture medium for three times, these cells were continuously cultured in bovine serum-free cell culture medium and were incubated with **Cy-OAcr** for 30 min. There no ratio signal were observed in Fig. 4a due to the intracellular Cys had been scavenged by NEM. Because the addition of exogenous Cys supplemented the intracellular Cys concentration (Fig. 4b), fluorescent images from Channel 2 emitted strong red fluorescence, and the fluorescence ratio signals were significantly increased compared to the absence of exogenous Cys (Fig. 3a). However, the addition of exogenous GSH-MEE did not contribute to the remarkable

changes in fluorescence (Fig. 4c). The similar results were obtained in the group d pretreated with exogenous Hcy (Fig. 4d). The mean ratios of group a, b, c, and d were displyed in Fig. 4e–h. On the basis of our findings, we confirmed that our probe **Cy-OAcr** could selectively utilize to detect intracellular Cys.

3.5. Detection of cysteine in tumor-bearing mice

Since the probe **Cy-OAcr** had successfully applied to the selective detection of Cys in cells, we next explored whether the probe could be used to detect Cys in vivo with the remarkable NIR optical properties. In vivo imaging of small animals system was used for the detection of Cys in tumor-bearing mice. The male nude mice (4 weeks old, ~20 g) in Fig. 5a were divided into six groups with bearing A549, H1650, PC9 cell lines tumor, respectively. After intratumorally injected **Cy-OAcr** for 1 h, the animals were subjected to in vivo imaging system for Cys detection. The fluorescent images in Fig. 5a were constructed from two fluorescence collection windows: Channel 1: λ_{ex} = 740 nm, λ_{em} = 750–830 nm; Channel 2: λ_{ex} = 520 nm, λ_{em} = 580–660 nm. Channel 2 (group a, b, and c) offered strong fluorescence from tumor lesion of the mice as the probe had detected Cys. However, when the mice in group I, II, and III were intratumorally preinjected NEM for to deplete all the biothiols in tumor lesion, the later injection of **Cy-OAcr** provided a dramatically decreasing intensity fluorescence image in
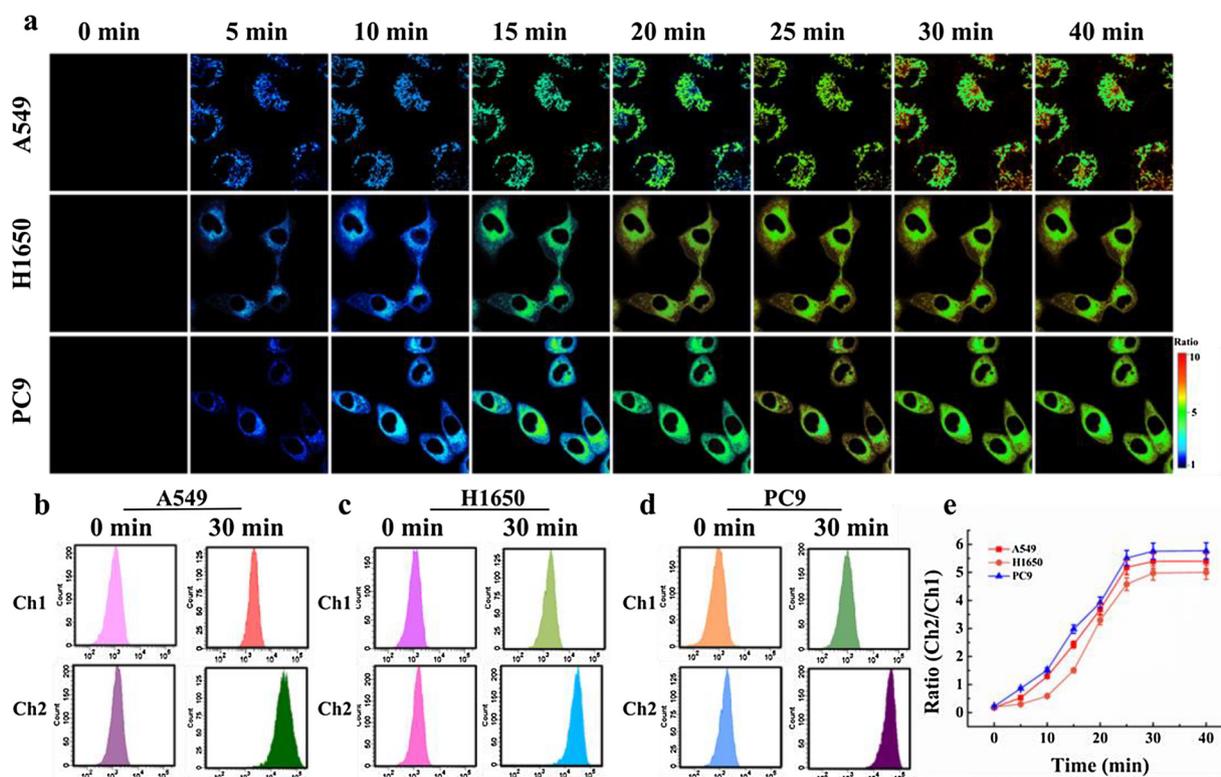
Fig. 3. Real-time ratio images and flow cytometry analysis endogenous Cys. a) Pseudocolor ratio images of endogenous Cys levels in A549, H1650 and PC9 cells at time points: 0, 5, 10, 15, 20, 25, 30 and 40 min. Fluorescence images collection windows for Channel 1: $\lambda_{ex} = 635$ nm, $\lambda_{em} = 700$–800 nm. Channel 2: $\lambda_{ex} = 550$ nm, $\lambda_{em} = 600$–700 nm. b) – d) Flow cytometry analysis of a). Channel 1: $\lambda_{ex} = 633$ nm, $\lambda_{em} = 750$–810 nm. Channel 2: $\lambda_{ex} = 488$ nm, $\lambda_{em} = 610$–670 nm. e) Plots of average ratio intensities of a). Ratios in e) were calculated through the fluorescence intensity ratio from Ch2/Ch1. The data were shown as mean (± s.d.) (n = 7).

Channel 2 compared to those mice without pretreatment of NEM. Fig. 5b illustrated the ratio of mean number of photons for each group shown in Fig. 5a. The above results confirmed that the NIR probe **Cy-OAcr** well behaved as the desirable candidate for detecting and imaging of Cys in complicated living organisms.

3.6. Detection of cysteine in orthotopic lung cancer mice

To verify the potential contribution of our probe **Cy-OAcr** for clinical auxiliary diagnosis, we performed further assays for the detection of Cys in the orthotopic lung cancer mice models. We used urethane to stimulate FVB mice to establish the orthotopic lung cancer mice model. The FVB mice were intraperitoneally injected with 8% urethane (dissolved in saline) at a dose of 0.01 ml g^{-1} twice a week. The whole
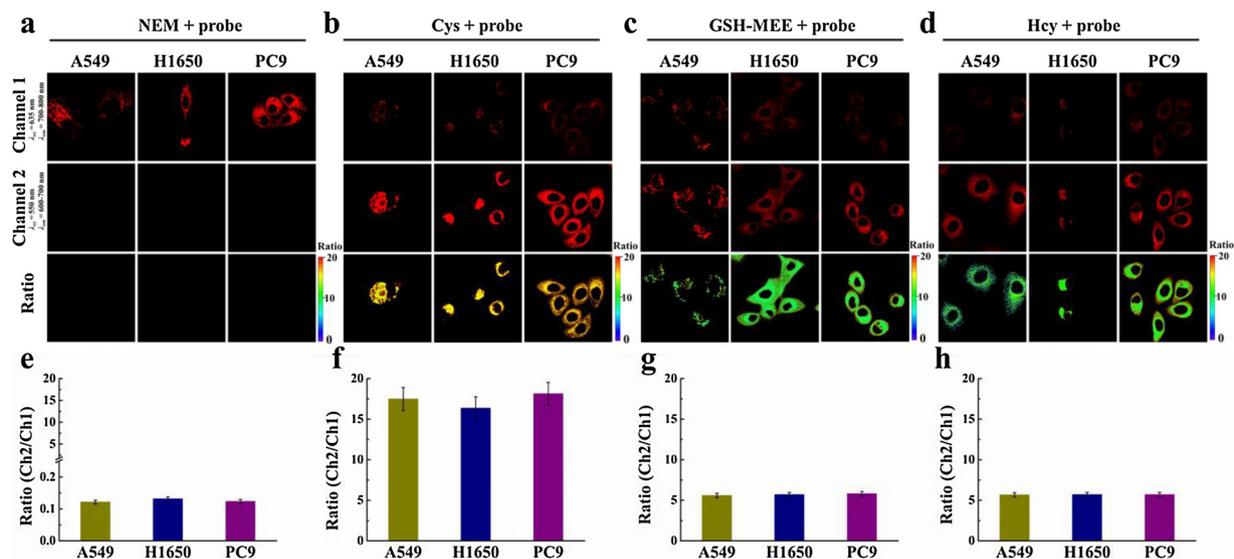

Fig. 4. Ratio images of the Cys in A549, H1650 and PC9 cells exposed to different stimulation agents. a) - d) The cells were pretreated with NEM (300 μM), Cys (200 μM), GSH-MEE (5 mM) and Hcy (200 μM) for 30 min and then incubated with **Cy-OAcr** (10 μM) for 30 min, respectively. Fluorescence images collection windows: Channel 1: $\lambda_{ex} = 635$ nm, $\lambda_{em} = 700$–800 nm. Channel 2: $\lambda_{ex} = 550$ nm, $\lambda_{em} = 600$–700 nm. e) - h) The average ratio fluorescence intensity of a) - d). Ratios in e) – h) were calculated through the fluorescence intensity ratio from Ch2/Ch1. The data were shown as mean (± s.d.) (n = 7).
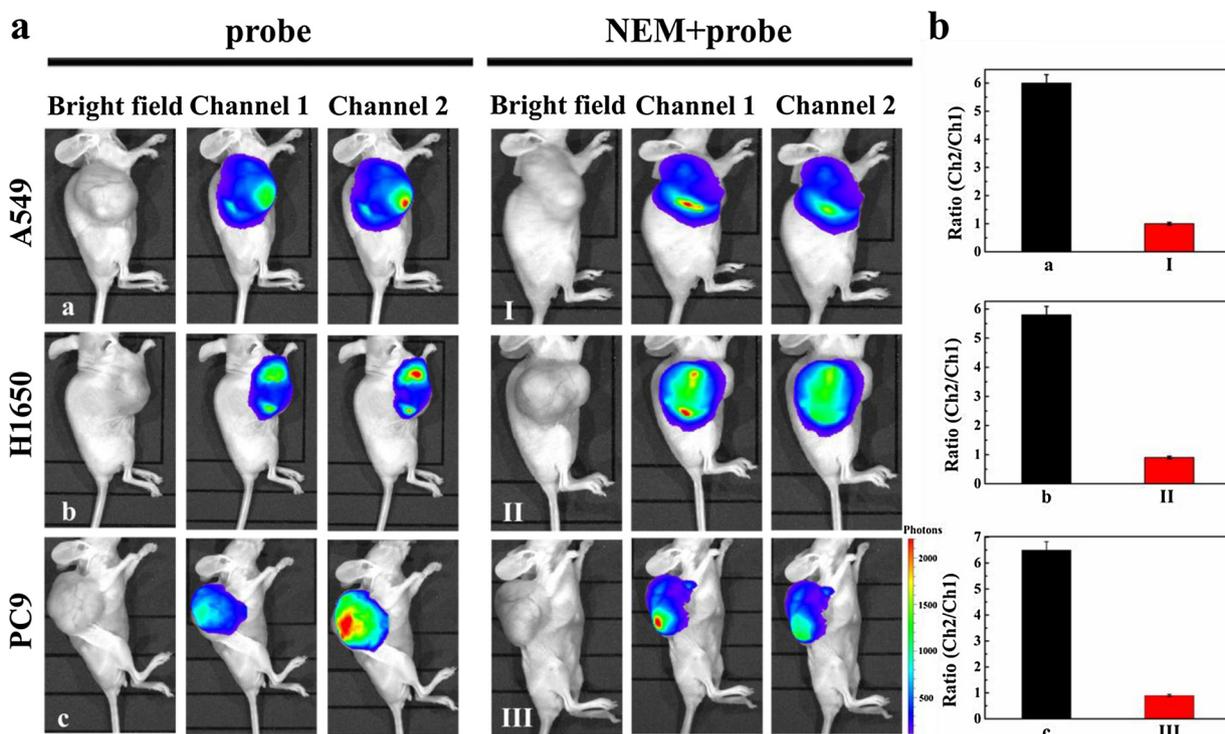
Fig. 5. In vivo imaging Cys in A549, H1650 and PC9 tumor-bearing mice. a) Group a, Group b and Group c were intratumorally injected **Cy-OAcr** (10 μM, 200 μl, in DMSO : saline = 1 : 99, v/v) for 1 h and then for in vivo imaging. Group I, Group II and Group III were intratumorally preinjected NEM (10 mM, 200 μL) for 1 h, subsequently injection of **Cy-OAcr** (10 μM, 200 μl, in DMSO : saline = 1 : 99, v/v) for 1 h, and then for in vivo imaging. The total number of photons from the entire tumor lesions of the mice were integrated. b) The average ratio intensity value of a). Ratios in b) were calculated through the mean number of photons ratio from Ch2/Ch1. The data were shown as mean (± s.d.) (n = 7).
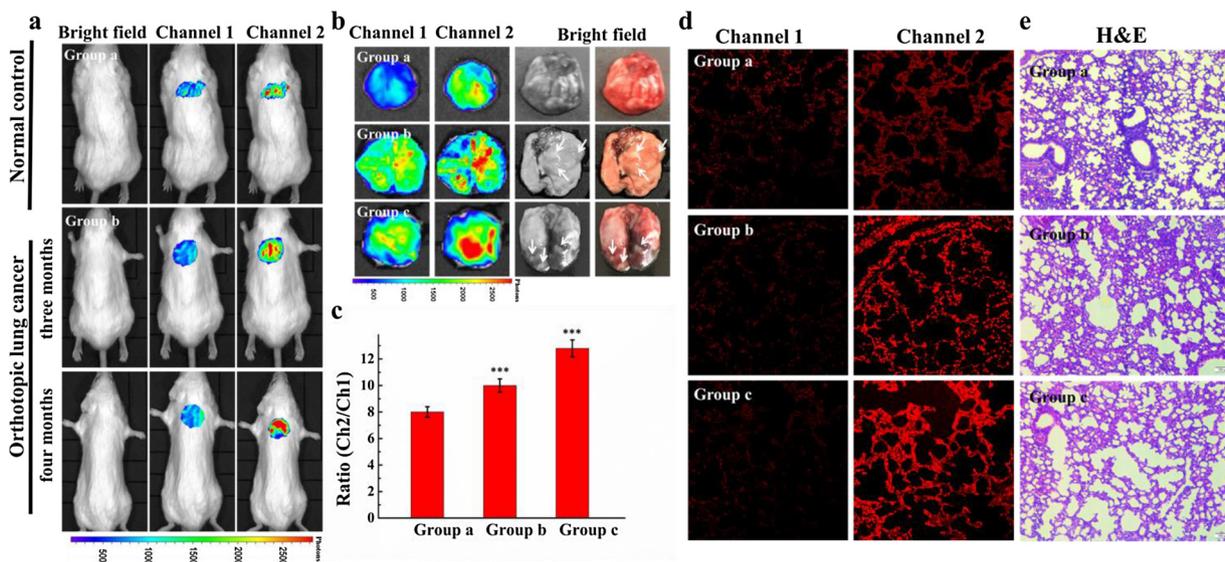

Fig. 6. In vivo imaging Cys in orthotopic lung cancer mice. a) In vivo fluorescent imaging. Fluorescence collection windows: Channel 1: λ_{ex} = 740 nm, λ_{em} = 750–830 nm. Channel 2: λ_{ex} = 520 nm, λ_{em} = 580–660 nm. b) Isolated lung fluorescence imaging. c) The average ratio intensity value of Group a–c at 30 min. Ratios in c) were calculated through the mean number of photons ratio from Ch2/Ch1. Difference was analyzed by one-way ANOVA and LSD post-test. ***P < 0.001 vs Group a. d) Confocal imaging of fresh lung tissue slice of Group a, b and c. Fluorescence images collection windows for Channel 1: λ_{ex} = 635 nm, λ_{em} = 700–800 nm. Channel 2: λ_{ex} = 550 nm, λ_{em} = 600–700 nm. Scale bar = 10 μm. e) H&E stained lung tissue from normal and cancer lesions in Group a–c. Scale bar = 20 μm. The data were shown as mean (± s.d.) (n = 7).

process consumed five weeks. Then it would take three months for the development of orthotopic lung cancer lesions. All the mice in Fig. 6a were administered **Cy-OAcr** (10 μM, 200 μl, in DMSO : saline = 1 : 99, v/v) through the tracheal spray. After 30 min, the mice were anesthetized with isoflurane for in vivo imaging. Normal mice in group a were as control. The orthotopic lung cancer mice model in group b were

three months, while the mice model in group c were four months. The results showed that the fluorescence intensity of Channel 2 in the lung cancer mice models was higher than that of the normal group, indicating the higher levles of Cys in the lung cancer mice models than in the normal mice. In the orthotopic lung cancer model group b and c, The fluorescence intensity of group c in Channel 2 was stonger than that

of in group b. The time-dependent quantization of fluorescence ratio was shown in Fig. 6c. In order to enable the diagnostic ability of our probe **Cy-OAcr,** all the mice were sacrificed after the performance of in vivo imaging. The isolated lungs were further underwent fluorescence imaging in vitro (Fig. 6b). The results were consistent with the results of in vivo imaging. Cancer lesions could be found in lung (arrows in bright fields of Fig. 6b). Obviously, cancer lesions emitted higher fluorescence than the normal lung tissue in Channel 2. The confocal images of the above-described fresh lung tissue sections were taken from confocal microscopy (Fig. 6d). The fluorescence intensities of the model group in Channel 2 were higher than the normal group. These results demonstrated that Cys concentration in tumor tissue were higher than that in normal tissue. We performed hematoxylin-eosin (H&E) pathological staining to verify the lung tissue (Fig. 6e). The result of H&E illustrated that nuclear atypia of group c was more clear than group b. This result also well explained why the fluorescence intensity in Channel 2 of group c was stronger than that of group b. Our results indicated that the probe **Cy-OAcr** had excellent ability to detect Cys in vivo. Given the high levels of Cys in tumor tissues, this new ratiometric NIR fluorescent probe had potentiality in the clinical auxiliary diagnosis of cancer.

4. Conclusions

In conclusion, based on previously research, we synthesize a ratiometric NIR fluorescent probe **Cy-OAcr** for highly selective detection of Cys from other structurally and functionally similar biothiols, such as GHS and Hcy. The rapid discrimination of Cys is based on an unique adduct/intramolecular cyclization reaction, which results in remarkable spectra shifts via modulating the conjugated π-electron system of cyanine fluorophore. The probe **Cy-OAcr** has low cytotoxicity and excellent membrane permeability. The probe preferentially accumulates within mitochondria and is capable of evaluating the levels of mitochondrial Cys in living cancer cell lines. Taking advantage of **Cy-OAcr**, we have achieved the detection and imaging of Cys in three tumor-bearing mice models. Moreover, this ratiometric NIR fluorescent probe has been successfully applied for bioimaging Cys in orthotopic lung cancer mice models. The results demonstrate that our probe has high potential for the clinical auxiliary diagnosis of cancer.

Acknowledgements

Appendix A. Supplementary data

Supplementary material related to this article can be found, in the online version, at doi:https://doi.org/10.1016/j.snb.2018.11.056.

References

[1] D.P. Jones, Y.M. Go, C.L. Anderson, T.R. Ziegler, Jr J.M. Kinkade, W.G. Kirlin, Cysteine/cystine couple is a newly recognized node in the circuitry for biologic redox signaling and control, FASEB J. 18 (2004) 1246–1248.

[2] X. Chen, Y. Zhou, X. Peng, J. Yoon, Fluorescent and colorimetric probes for detection of thiols, Chem. Soc. Rev. 39 (2010) 2120–2135.

[3] M. Guichard, F. Lespinasse, R. Estelin, A. Gerbaulet, C. Haie, E. Lartigau, E.P. Malaise, C. Micheau, M. Prade, J.M. Richard, P. Weeger, Glutathione and cysteine levels in human tumour biopsies, Br. J. Radiol. 63 (1990) 557–561.

[4] S.M. Evans, R. Lew, M.L. Kochman, E.P. Wileyto, E. Baum, K.M. Safford, C.J. Koch, Human esophageal cancer is distinguished from adjacent esophageal tissue by tissue cysteine concentrations, Dig. Dis. Sci. 47 (2002) 2743–2750.

[5] L. Yuan, W. Lin, Y. Yang, A ratiometric fluorescent probe for specific detection of cysteine over homocysteine and glutathione based on the drastic distinction in the kinetic profiles, Chem. Commun. 47 (2011) 6275–6277.

[6] J. Liu, Y. Sun, Y. Huo, H. Zhang, L. Wang, P. Zhang, D. Song, Y. Shi, W. Guo, Simultaneous fluorescence sensing of cys and GSH from different emission channels, J. Am. Chem. Soc. 136 (2014) 574–577.

[7] X. Jiang, J. Chen, A. Bajić, C. Zhang, X. Song, S.L. Carroll, Z.L. Cai, M. Tang, M. Xue, N. Cheng, C.P. Schaaf, F. Li, K.R. MacKenzie, A.C.M. Ferreon, F. Xia, M.C. Wang, M.M. Maletić-Savatić, J. Wang, Quantitative real-time imaging of glutathione, Nat. Commun. 8 (2017) 16163–16174, https://doi.org/10.1038/ncomms16087.

[8] J. Vacek, B. Klejdus, J. Petrlová, L. Lojková, V. Kubán, A hydrophilic interaction chromatography coupled to a mass spectrometry for the determination of glutathione in plant somatic embryos, Analyst 131 (2006) 1167–1174.

[9] A.P. Vellasco, R. Haddad, M.N. Eberlin, N.F. Höehr, Combined cysteine and homocysteine quantitation in plasma by trap and release membrane introduction mass spectrometry, Analyst 127 (2002) 1050–1053.

[10] B. Seiwert, U. Karst, Simultaneous LC/MS/MS determination of thiols and disulfides in urine samples based on differential labeling with ferrocene-based maleimides, Anal. Chem. 79 (2007) 7131–7138.

[11] J.O. Escobedo, W. Wang, R.M. Strongin, Use of a commercially available reagent for the selective detection of homocysteine in plasma, Nat. Protoc. 1 (2006) 2759–2762.

[12] J.S. Stamler, J. Loscalzo, Capillary zone electrophoretic detection of biological thiols and their S-nitrosated derivatives, Anal. Chem. 64 (1992) 779–785.

[13] T. Inoue, J.R. Kirchhoff, Determination of thiols by capillary electrophoresis with amperometric detection at a coenzyme pyrroloquinoline quinone modified electrode, Anal. Chem. 74 (2002) 1349–1354.

[14] C. Yin, K. Xiong, F. Huo, J.C. Salamanca, R.M. Strongin, Fluorescent probes with multiple binding sites to distinguish Cys, Hcy and GSH, Angew. Chem. 56 (2017) 13188–13198.

[15] X. Li, X. Gao, W. Shi, H. Ma, Design strategies for water-soluble small molecular chromogenic and fluorogenic probes, Chem. Rev. 114 (2013) 590–659.

[16] H. Liu, K. Li, X. Hu, L. Zhu, Q. Rong, Y. Liu, X. Zhang, J. Hasserodt, F. Qu, W. Tan, In situ localization of enzyme activity in live cells by a molecular probe releasing a precipitating fluorochrome, Angew. Chem. 56 (2017) 11788–11792.

[17] H.S. Jung, J.H. Han, T. Pradhan, S. Kim, S.W. Lee, J.L. Sessler, T.W. Kim, C. Kang, J.S. Kim, A cysteine-selective fluorescent probe for the cellular detection of cysteine, Biomaterials 33 (2017) 945–953.

[18] C. Han, H. Yang, M. Chen, Q. Su, W. Feng, F. Li, Mitochon-dria-targeted near-infrared fluorescent off-on probe for selective detection of cysteine in living cells and in vivo, ACS Appl. Mater. Interfaces 7 (2015) 27968–27975.

[19] T. Liu, F. Huo, J. Li, J. Chao, Y. Zhang, C. Yin, An off-on fluorescent probe for specifically detecting cysteine and its application in bioimaging, Sens. Actuators B: Chem. 237 (2016) 127–132.

[20] Y.H. Lee, W.X. Ren, J. Han, K. Sunwoo, J.Y. Lim, J.H. Kim, J.S. Kim, Highly selective two-photon imaging of cysteine in cancerous cells and tissues, Chem. Commun. 51 (2015) 14401–14404.

[21] X. Dai, Q. Wu, P. Wang, J. Tian, Y. Xu, S. Wang, J. Miao, B. Zhao, A simple and effective coumarin-based fluorescent probe for cysteine, Biosens. Bioelectron. 59 (2014) 35–39.

[22] J. Liu, Y. Sun, H. Zhang, Y. Huo, Y. Shi, H. Shi, W. Guo, A carboxylic acid-functionalized coumarinhemicyanine fluorescent dye and its application to construct a fluorescent probe for selective detection of cysteine over homocysteine and glutathione, RSC Adv. 4 (2014) 64542–64550.

[23] S. Li, Y. Fu, C. Li, Y. Li, L. Yi, J. Yang, A near-infrared fluorescent probe based on BODIPY derivative with high quantum yield for selective detection of exogenous and endogenous cysteine in biological samples, Anal. Chim. Acta 994 (2017) 73–81.

[24] L. He, X. Yang, K. Xu, X. Kong, W. Lin, A multi-signal fluorescent probe for simultaneously distinguishing and sequentially sensing cysteine/homocysteine, glutathione, and hydrogen sulfide in living cells, Chem. Sci. 8 (2017) 6257–6265.

[25] H. Zhang, R. Liu, J. Liu, L. Li, P. Wang, S. Yao, Z. Xu, H. Sun, A minimalist fluorescent probe for differentiating Cys, Hcy and GSH in live cells, Chem. Sci. 7 (2016) 256–260.

[26] X. Yang, L. He, K. Xu, W. Lin, A fluorescent dyad with large emission shift for discrimination of cysteine/homocysteine from glutathione and hydrogen sulfide and the application of bioimaging, Anal. Chim. Acta 981 (2017) 86–93.

[27] M. Jia, L. Niu, Y. Zhang, Q. Yang, C.H. Tung, Y. Guan, L. Feng, BODIPY-based fluorometric sensor for the simultaneous determination of Cys, Hcy, and GSH in human serum, ACS Appl. Mater. Interfaces 7 (2015) 5907–5914.

[28] F. Wang, Z. Guo, X. Li, X. Li, C. Zhao, Development of a small molecule probe capable of discriminating cysteine, homocysteine, and glutathione with three distinct turn-on fluorescent outputs, Chem.-Eur. J. 20 (2014) 11471–11478.

[29] X. Liu, L. Niu, Y. Chen, Y. Yang, Q. Yang, A multi-emissive fluorescent probe for the discrimination of glutathione and cysteine, Biosens. Bioelectron. 90 (2017) 403–409.

[30] M. Zhang, M. Yu, F. Li, M. Zhu, M. Li, Y. Gao, L. Li, Z. Liu, J. Zhang, D. Zhang, T. Yi, C. Huang, A highly selective fluorescence turn-on sensor for cysteine/homocysteine and its application in bioimaging, J. Am. Chem. Soc. 129 (2007) 10322–10323.

[31] F. Wang, J. An, L. Zhang, C. Zhao, Construction of a fluorescence turn-on probe for highly discriminating detection of cysteine, RSC Adv. 4 (2014) 53437–53441.

[32] D. Su, C.L. Teoh, S. Sahu, R.K. Das, Y.T. Chang, Live cells imaging using a turn-on FRET-based BODIPY probe for biothiols, Biomaterials 35 (2014) 6078–6085.

[33] H.Y. Shiu, H.C. Chong, Y.C. Leung, M.K. Wong, C.M. Che, A highly selective FRET-based fluorescent probe for detection of cysteine and homocysteine, Chem.-Eur. J. 16 (2010) 3308–3313.

[34] L. He, X. Yang, K. Xu, W. Lin, Improved aromatic substitu-tion-rearrangement-based

ratiometric fluorescent cyste-ine-specific probe and its application of real-time imaging under oxidative stress in living zebrafish, Anal. Chem. 89 (2017) 9567–9573.

[35] W. Fan, X. Huang, X. Shi, Z. Wang, Z. Lu, C. Fan, Q. Bo, A simple fluorescent probe for sensing cysteine over homocysteine and glutathione based on PET, Spectrochim. Acta A: Mol. Biomol. Spectrosc. 173 (2017) 918–923.

[36] C. Chen, W. Liu, C. Xu, W. Liu, A colorimetric and fluorescent probe for detecting intracellular biothiols, Biosens. Bioelectron. 85 (2016) 46–52.

[37] Y. Tang, L. Jin, B. Yin, A dual-selective fluorescent probe for GSH and Cys detection: emission and pH dependent selectivity, Anal. Chim. Acta 993 (2017) 87–95.

[38] B.K. Rani, S.A. John, A novel pyrene based fluorescent probe for selective detection of cysteine in presence of other bio-thiols in living cells, Biosens. Bioelectron. 83 (2016) 237–242.

[39] C. Zhang, G. Zhang, L. Feng, J. Li, A ratiometric fluorescent probe for sensitive and selective detection of hydrogen sulfide and its application for bioimaging, Sens. Actuators B: Chem. 216 (2015) 412–417.

[40] J. Mei, Y. Wang, J. Tong, J. Wang, A. Qin, J. Sun, B. Tang, Discriminatory detection of cysteine and homocysteine based on dialdehyde-functionalized aggregation-induced emission fluorophores, Chem.-Eur. J. 19 (2013) 613–620.

[41] L. Bu, J. Chen, X. Wei, X. Li, H. Ågren, Y. Xie, An AIE and ICT based NIR florescent probe for cysteine and homocysteine, Dyes Pigm. 136 (2017) 724–731.

[42] Z. Chen, Q. Sun, Y. Yao, X. Fan, W. Zhang, J. Qian, Highly sensitive detection of cysteine over glutathione and homo-cysteine: new insight into the Michael addition of mercapto group to maleimide, Biosens. Bioelectron. 91 (2017) 553–559.

[43] M. Hu, J. Fan, H. Li, K. Song, S. Wang, G. Cheng, X. Peng, Fluorescent chemodosimeter for Cys/Hcy with a large absorption shift and imaging in living cells, Org. Biomol. Chem. 9 (2011) 980–983.

[44] S. Wang, Q. Wu, H. Wang, X. Zheng, S. Shen, Y. Zhang, J. Miao, B. Zhao, A novel pyrazoline-based selective fluorescent probe for detecting reduced glutathione and its application in living cells and serum, Analyst 138 (2013) 7169–7174.

[45] Z. Fu, X. Han, Y. Shao, J. Fang, Z. Zhang, Y. Wang, Y. Peng, Fluorescein-based chromogenic and ratiometric fluorescence probe for highly selective detection of cysteine and its application in Bioimaging, Anal. Chem. 89 (2017) 1937–1944.

[46] R.R. Nawimanage, B. Prasai, S.U. Hettiarachchi, R.L. McCarley, Cascade reaction-based, near-infrared multiphoton fluorescent probe for the selective detection of cysteine, Anal. Chem. 89 (2017) 6886–6892.

[47] W. Lin, L. Long, L. Yuan, Z. Cao, B. Chen, W. Tan, A ratiometric fluorescent probe for cysteine and homocysteine displaying a large emission shift, Org. Lett. 10 (2008) 5577–5580.

[48] C.Y. Kim, H.J. Kang, S.J. Chung, H.K. Kim, S.Y. Na, H.J. Kim, Mitochondria-targeting chromogenic and fluorescence turn-on probe for the selective detection of cysteine by caged oxazolidinoindocyanine, Anal. Chem. 88 (2016) 7178–7182.

[49] F. Wang, L. Zhou, C. Zhao, R. Wang, Q. Fei, S. Luo, Z. Guo, H. Tian, W. Zhu, A dual-response BODIPY-based fluorescent probe for the discrimination of glutathione from cystein and homocysteine, Chem. Sci. 6 (2015) 2584–2589.

[50] J.V. Frangioni, In vivo near-infrared fluorescence imaging, Curr. Opin. Chem. Biol. 7 (2003) 626–634.

[51] Z. Guo, S. Park, J. Yoon, I. Shin, Recent progress in the development of near-infrared fluorescent probes for bioimaging applications, Chem. Soc. Rev. 43 (2014) 16–29.

[52] C. Zhao, X. Li, F. Wang, Target-triggered NIR emission with a large stokes shift for the detection and imaging of cysteine in living cells, Chem. – An Asian J. 9 (2014) 1777–1781.

[53] T. Ueno, T. Nagano, Fluorescent probes for sensing and imaging, Nat. Methods 8 (2011) 642–645.

[54] L. Niu, Y. Guan, Y. Chen, L. Wu, C. Tung, Q. Yang, BODIPY-based ratiometric fluorescent sensor for highly selective detection of glutathione over cysteine and homocysteine, J. Am. Chem. Soc. 134 (2012) 18928–18931.

[55] Z. Guo, S. Nam, S. Park, J. Yoon, A highly selective ratiometric near-infrared fluorescent cyanine sensor for cysteine with remarkable shift and its application in bioimaging, Chem. Sci. 3 (2012) 2760–2765.

[56] Y. Li, Y. Sun, J. Li, Q. Su, W. Yuan, Y. Dai, C. Han, Q. Wang, W. Feng, F. Li, Ultrasensitive near-infrared fluorescence-enhanced probe for for in vivo nitroreductase imaging, J. Am. Chem. Soc. 137 (2015) 6407–6416.

[57] F. Yu, M. Gao, M. Li, L. Chen, A dual response near-infrared fluorescent probe for hydrogen polysulfides and superoxide anion detection in cells and in vivo, Biomaterials 63 (2015) 93–101.

[58] G.T. Stathopoulos, T.P. Sherrill, D.S. Cheng, R.M. Scoggins, W. Han, V.V. Polosukhin, L. Connelly, F.E. Yull, B. Fingleton, T.S. Blackwell, Epithelial NF-kappaB activation promotes urethane-induced lung carcinogenesis, Proc. Natl. Acad. Sci. U. S. A. 104 (2007) 18514–18519.

[59] K. Yin, F. Yu, W. Zhang, L. Chen, A near-infrared ratiometric fluorescent probe for cysteine detection over glutathione indicating mitochondrial oxidative stress in vivo, Biosens. Bioelectron. 74 (2015) 156–164.

[60] S. Luo, X. Tan, S. Fang, Y. Wang, T. Liu, X. Wang, Y. Yuan, H. Sun, Q. Qi, C. Shi, Mitochondria-targeted small-molecule fluorophores for dual modal cancer photo-therapy, Adv. Funct. Mater. 26 (2016) 2826–2835.

[61] Y. Qi, Y. Huang, B. Li, F. Zeng, S. Wu, Real-time monitoring of endogenous cysteine levels in vivo by near-infrared turn-on fluorescent probe with large stokes shift, Anal. Chem. 90 (2017) 1014–1020, https://doi.org/10.1021/acs.analchem.7b04407.

[62] P. Blondeau, R. Gauthier, C. Berse, D. Gravel, Synthesis of some stable 7-Halo-1,4-thiazepines, Can. J. Chem. 49 (1971) 3866–3876.

[63] Y. Yue, F. Huo, X. Li, Y. Wen, T. Yi, J. Salamanca, J.O. Escobedo, R.M. Strongin, C. Yin, pH-Dependent fluorescent probe that can be tuned for cysteine or homo-cysteine, Org. Lett. 19 (2017) 82–85.

[64] X. Yang, Y. Guo, R.M. Strongin, Conjugate additionclization sequence enables selective and simultaneous fluorescence detection of cysteine and homocysteine, Angew. Chem. – Int. Ed. 50 (2011) 10690–10693.

[65] F. Kong, R. Liu, R. Chu, X. Wang, K. Xu, B. Tang, A highly sensitive near-infrared fluorescent probe for cysteine and homocysteine in living cells, Chem. Commun. 49 (2013) 9176–9178.

[66] L. Strekowski, M. Lipowska, G. Patonay, Facile derivattlations of heptamethine cyanine dyes, Synth. Commun. 22 (1992) 2593–2598.

[67] D.W. Bak, E. Weerapan, Cysteine-mediated redox signalling in the mitochondria, Mol. Biosyst. 11 (2015) 678–697.

[68] J. Palmfeldt, P. Bross, Proteomics of human mitochondria, Mitochondrion 33 (2017) 2–14.

[69] G. Giachin, R. Bouverot, S. Acajjaoui, S. Pantalone, M. Soler-López, Dynamics of human mitochondrial complex I assembly: implications for neurodegenerative diseases, Front. Mol. Biosci. 3 (2016) 1–20.

Xiaoyu Zhang is currently a physician at Yantai Affiliated Hospital of Binzhou Medical University. She received her master candidate, joint-educated, at Binzhou Medical University, and Yantai Institute of Coastal Zone Research, Chinese Academy of Sciences, during 2015 - 2018. She received her BS from Binzhou Medical University, in 2015. Her current research interest is focused on the accurate diagnosis of pulmonary fibrosis and lung cancer.

Na He is currently a master candidate, joint-educated, at Binzhou Medical University, and Yantai Institute of Coastal Zone Research, Chinese Academy of Sciences, since 2017. She received her BS from Binzhou Medical University, in 2017. Her current interest in research focuses on bioimaging.

Yan Huang is currently a PhD candidate, joint-educated, at Shandong Normal University, and Yantai Institute of Coastal Zone Research, Chinese Academy of Sciences, since 2016. His research interests focus on functional fluorescent probe, theranostics, and functional nanomaterial.

Fabiao Yu is currently a professor at Institute of Functional Materials and Molecular Imaging, Hainan Medical University. He served for Yantai Institute of Coastal Zone Research, Chinese Academy of Sciences during 2013 - 2017. He received his PhD, joint-educated, at Dalian University of Technology, and Dalian Institute of Chemical Physics, Chinese Academy of Sciences, in 2013. His research interests focus on functional probe molecules (fluorescence and phosphorescence analysis), theranostics, and organic functional materials.

Bowei Li is currently as an associate professor at Yantai Institute of Coastal ZoneResearch, Chinese Academy of Sciences. He received his pH.D. at Dalian Institute of Chemical Physics, Chinese Academy of Sciences, in 2009. During 2009–2011, he worked at Department of Chemistry, Florida State University. His research interests focus on the environmental monitoring, point-of-care testing, and other fields of basic research on chemical and biological using microfluidic chip platform.

Changjun Lv is now a vice president in Binzhou Medical University. He is a professor and serves in Affiliated Hospital of Binzhou Medical University as a chief physician. He received his MD from China Medical University in 1995. He is skilled in the diagnosis and treatment of respiratory diseases, especially in the diagnosis of interstitial lung diseases. He is an expert with China's State Council special allowance due to his excellent performance in clinical work. His research interests include diagnosis and therapy of idiopathic pulmonary fibrosis, drug developments, and theranostics.

Lingxin Chen has been a professor at Yantai Institute of Coastal Zone Research, Chinese Academy of Sciences, since 2009. He obtained his pH.D. in analytical chemistry at Dalian Institute of Chemical Physics, Chinese Academy of Sciences, in 2003. During 2004–2009, he worked at Department of Chemistry, Tsinghua University, and Department of Applied Chemistry, Hanyang University, respectively. His research interests include the studies of novel properties of materials such as functionalized nanoparticles & functional probe molecules for developing nanoscale biochemical analysis methods and molecular imprinting-based sample pretreatment technology.